Debye-Waller factors of alkali halides

C. K. Shepard* and J. G. Mullen
Purdue University, West Lafayette, Indiana 47907-1396

G. Schupp
University of Missouri Research Reactor, Columbia, Missouri 65211

(Received 8 August 1997)

Using very-high-intensity ($\sim$70 Ci) ^{183}Ta Mössbauer sources, we have measured the Debye-Waller factors (DWF's) of sodium chloride, potassium chloride, and potassium bromide single crystals for several of the $(h00)$ and (nnn) Bragg reflections. We have used an approach which properly accounts for thermal expansion over the temperature range of our experiment, from 90 K to 900 K, about 100 K below the melting point of our crystals. We have found that a procedure used to analyze data by earlier workers leads to incorrect parameters in the Debye-Waller factor exponent, and our procedure does not require empirical parameters to account for the effects of thermal expansion. Additionally, we find three items of significance. Contrary to earlier results, we observe that the cations and the anions have identical DWF's in NaCl and also in KBr. We observe terms in the expansion of the DWF exponential which are quartic in the scattering wave vector $\vec{Q}$ in NaCl and KCl, with some evidence for a Q^4 term in KBr. The size of the Q^4 contribution is reported and varies with the direction of momentum transfer. We also observe that the Debye temperature and the coefficient of the anharmonic Q^2 term also vary with the direction of momentum transfer. We believe our data are the definitive evidence for a nonspherical thermal cloud in a cubic crystal; the ions have a larger amplitude of oscillation in the $[h00]$ direction than in the $[nnn]$ direction, contrary to the commonly held view of crystallographers that the most general form of the mean-square thermal motion is of an ellipsoid shape. [S0163-1829(98)03602-9]

I. INTRODUCTION

The reduction in elastic scattering of photons by the thermal motion of atoms in a crystal is characterized by the Debye-Waller factor (DWF). It is given by

$$\mathrm{DWF} = e^{-2M} = |\langle e^{i\vec{Q}\cdot\vec{u}_l}\rangle|^2, \tag{1}$$

where $\vec{Q}$ is the scattering wave vector and $\vec{u}_l$ is the displacement from equilibrium of the lth ion in the basis. Its temperature dependence provides a method for examining the lattice dynamics of a crystal, including the anharmonic terms of the lattice potential. The measurement of the Debye-Waller factor of single crystals, as a function of temperature, is complicated by thermal diffuse scattering and by thermal expansion of the sample crystal. Thermal diffuse scattering (TDS) is inelastic scattering due to lattice phonons. Since the DWF characterizes the elastic scattering, the inelastic scattering must first be removed from the total scattering intensity. The thermal expansion of the crystal creates difficulties in carrying out the experiments and in properly analyzing the data as the scattering vectors and the number of scattering sites illuminated by the incident beam vary with temperature. The high-energy resolution of Mössbauer radiation allows us to distinguish between elastic and inelastic scattering, and we have carefully corrected for the effects of thermal expansion (measured by earlier workers), allowing us to make very accurate measurements of the DWF for NaCl, KCl, and KBr.

It is important to experimentally separate the elastic and inelastic scattering from the sample crystal. To observe anharmonic effects, we must make measurements at high temperatures and for higher-order Bragg reflections. At low temperatures and for the lowest-order reflections, TDS is a small fraction of the total scattering and so a poor estimate of the amount of TDS will not greatly affect the DWF. However, as the temperature of the sample approaches the melting temperature, the TDS can dominate the elastic scattering for (600) and higher-order reflections. In these cases, a good experimental measurement of TDS is required to avoid a systematic bias due to theoretical estimates of the TDS. Since the energy change in the scattered photon is small, $\sim$10 meV, standard x-ray techniques are unable to distinguish the elastic scattering from the inelastic scattering. This may be accomplished by using the high-energy resolution of the Mössbauer effect.

By using a Mössbauer γ-ray source, the TDS can be measured experimentally and the elastic intensity can be obtained. The resonant photons from the 46.5-keV Mössbauer level in ^{183}W (produced by the decay of ^{183}Ta) have an energy width of 2.5 μeV. A resonant photon which is inelastically scattered by the crystal will have its energy shifted by an amount of the order of 10 meV, making it nonresonant with the 46.5-keV Mössbauer effect transition which is detectable when it is analyzed by a Mössbauer absorber foil. Since the energy width of the Mössbauer line is of the order of 10^{-3} times the phonon energy, the probability of a nonresonant photon being scattered into the resonant window for absorption is negligible. Any TDS in the scattering crystal, therefore, lowers the observed resonant fraction of the beam on scattering. The recoilless fraction of the beam before scattering may be measured by Doppler-shifting the absorber in the beam before scattering from the crystal (putting the absorber between the source and the sample); the recoilless

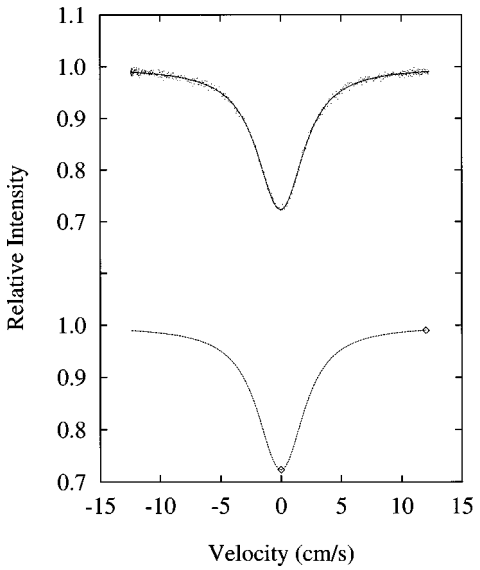

FIG. 1. Comparison of Mössbauer spectra. The upper spectrum is the full Mössbauer spectrum collected in this experiment. The lower spectrum is a two-point, on- and off-resonance spectrum similar to those collected by earlier researchers.

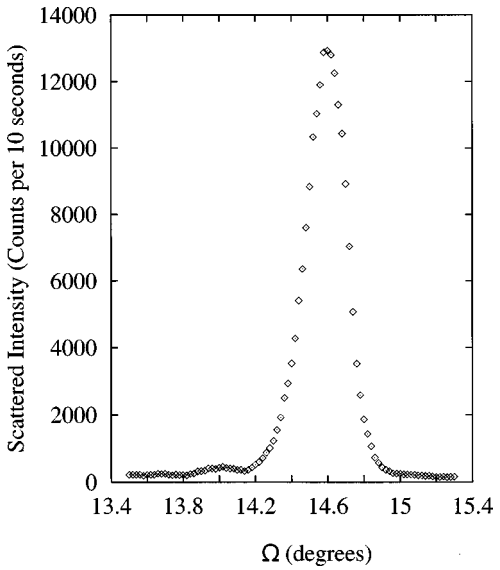

FIG. 2. Rocking curves for potassium chloride at room temperature.

fraction after scattering may be measured by moving the absorber to a position between the sample and the detector.

Measurement of Debye-Waller factors by this method has been hindered by the low intensity of typical Mössbauer sources. The typical ~100-mCi ^{57}Co source requires very close geometry with large acceptance angles and uses only two points on the Mössbauer spectrum (on and off resonance) to determine the elastic fraction.[1–6] Typically, the distance from source to detector is on the order of 25 cm, with acceptance angles of several degrees, leading to cosine smearing of the spectrum. These sources are widely used for other purposes because of their much greater energy resolution, only 4.7 neV; however, the resolution of the ^{183}Ta sources is more than adequate to resolve the differences in energy due to phonon interactions and these sources can be manufactured with far greater photon intensity in the Mössbauer transition. We have utilized these ^{183}Ta supersources available at the University of Missouri Research Reactor (MURR) to make accurate measurements of the DWF. The increase in intensity (of a factor of about 500 in Mössbauer photons) allows us to collect full Mössbauer spectra rather than two-point spectra (see Fig. 1) and to collimate our beam to about 0.3°.[7] In addition, it allows us to fit our spectra to the true line shape of the transition, rather than assuming a Lorentzian shape, which leads to errors in the measured elastic scattering fraction in on- and off-resonance measurements and even erroneous Debye temperatures.[8–14] As a source decays, absorber nuclei build up in the source, and source resonance self-absorption (SRSA) begins to distort the shape of the observed Mössbauer line. We used sources for only 1 week, during which SRSA is negligible. However, over the lifetime of a ^{57}Co source, the observed source recoilless fraction can change by more than 30%, changing the line shape and distorting the measurements of elastic scattering fraction.[15] By collecting full Mössbauer spectra, fitting them to the true line shape, and using sources only for a short period of time, we have eliminated these common sources of systematic error from our experiments.

II. EXPERIMENTAL METHOD AND APPARATUS

The experiments on three alkali halides were carried out at MURR using the Mössbauer facility.[7] The reactor produces very intense ^{183}Ta sources weekly. These sources are transferred into a stationary cask for the presently reported Mössbauer diffraction studies. This instrument consists of a stationary, heavily shielded source cask, a rotary stage for crystal scattering which accommodates either a furnace or a cryostat, an oscillating stage for the Mössbauer absorbers, and a solid-state photon detector. The sample stage and the detector table, which holds the detector and the oscillating stage, are driven by computer, allowing control of Θ and 2Θ (the orientation of the sample crystal and the scattering angle). The distance between the source and the detector is approximately 1.5 m.

The γ-ray beam is collimated to 1 in. in height and 0.125 in. in width before reaching the sample crystal. For the lowest-order reflections it is possible to collimate the beam to 0.0625 in. in width if needed. After scattering from the sample crystal, the beam passes through a 1 in. by 0.5 in. opening before reaching the detector. The extra width allows the entire scattered beam to be detected. (The scattered beam is wider than the incident beam due to penetration into the sample crystal; we choose to accept the entire scattered beam so that thermal expansion corrections are simplified.)

We used NaCl and KBr crystals fabricated by Bicron, Inc. These crystals were grown and cut so that the desired Bragg planes were parallel to the crystal face. We obtained two crystals for each salt, one oriented on the $[h00]$ and one on the $[nnn]$. These crystals were nominally $2.5\times1.2\times0.125$ in. The length of the crystals allowed the entire photon beam to illuminate part of the crystal face and scatter in reflection geometry. These crystals had rocking curves with a full width at half maximum of less than 0.5°; a typical rocking curve (ω scan) is shown in Fig. 2. Bicron also fabricated

KCl crystals, but these had large mosaic spreads; other KCl crystals were obtained from the University of Utah. These crystals were much smaller, so that the entire crystal was bathed by the photon beam. Some data were taken using the larger crystals; the same results were obtained in each case.

The temperature of the sample crystals was adjusted from about 90K to room temperature by using a liquid nitrogen Dewar. The sample crystals, in a boron nitride holder, are placed in an isothermal holder which is attached to a cold finger. There is a thermal switch which may be evacuated to inhibit heat transfer between the sample and the nitrogen bath when the sample is being heated above nitrogen temperatures by small rod heaters. The temperature is controlled by a thermocouple and measured by two platinum resistors located on the isothermal holder.

Above room temperature the temperature of the sample crystals may be heated up to near their respective melting points by the use of a furnace. The sample crystals, in a boron nitride holder, are placed in an isothermal copper holder, with 1-mil copper end windows for the beam to pass through, which is between two heating coils. There are five thermocouples used for temperature control and measurement of temperature. At even the highest temperatures the temperature variation was less than 3°, and usually the temperature was constant within 1°. The outside of the furnace is water cooled, and there are up to four tantalum heat shields surrounding the sample, with windows cut out for beam transmission.

We wanted to collect data as near to the melting points of the crystals as possible (the melting points of the crystals are 1074 K for NaCl, 1043 K for KCl, and 1007 K for KBr); however, at temperatures near the melting point the alkali-halide crystals tended to evaporate excessively. This had two effects; the crystal gradually became thinner, moving the position of the crystal face away from the γ-ray beam, and depositing the evaporated material on the window foils, attenuating the intensity of the transmitted beam. To overcome this problem we reduced the maximum temperature to which we raised our crystals and we coated the crystals with colloidal graphite. The coating of carbon did not affect the diffraction peaks, but it did reduce the evaporation problem, eliminating it completely below 850 K. At and above 850 K there was evidence of some small amount of evaporation occurring; we monitored the drop in count rate caused by evaporated material depositing on the copper windows and corrected for this effect, but it did introduce additional uncertainty into these very highest data points.

At each temperature it was necessary to align the sample crystal in the gamma-ray beam. Due to the thermal expansion of the crystal and furnace or cryostat, the position of the crystal relative to the beam changed slightly each time the sample temperature was changed. Aligning the crystal was accomplished by a hand-driven screw which translated the crystal into and out of the beam. This alignment process introduced the largest, nonstatistical uncertainty into the data. For the lowest-order reflections, this is very significant. For the higher-angle reflections, the actual changes in intensity with temperature were large, so that a small variation is less important. Also, it was at low angles that the beam size was nearly the same as the crystal size; the high-angle reflections were much less sensitive to the alignment of the crystal in the beam.

At each temperature we examined the rocking curves (ω scan) of each Bragg peak and collected a Mössbauer spectrum after scattering from each peak. In this way we measured the total intensity (elastic plus inelastic) of each reflection and determined the elastic scattering fraction for each reflection. We oscillated a resonant absorber, a natural tungsten foil 2 mils thick, between the sample crystal and the detector. A line shape analysis of each Mössbauer spectrum, based on an analytic expansion of the transmission integral,[8–12] determined the recoilless fraction of the photon beam after scattering from the sample. The Mössbauer line shape depends on the thickness of the absorber, the SRSA in the source, the recoilless fraction of the source, the width of the transition, and the number of counts collected. The thickness of the absorber and the SRSA were taken as known values from previous high-precision measurements.[11,12] Additionally, we have shown that, provided the actual absorber thickness and SRSA are constant, the elastic scattering fraction does not change for small inaccuracies in the thickness number of the absorber or the source. That is, using a slightly inaccurate value for one of these parameters will affect the recoilless fraction measured in both the before and after positions, but the elastic scattering fraction will be unaffected. We also took the width of the transition ($\hbar/\tau$, where τ is the lifetime of the excited state) to be known, after confirming that there was no instrumental broadening. In this manner, we reduced the number of parameters to avoid parameter correlation problems in fitting these spectra.

To measure the recoilless fraction of the photon beam before scattering, we used a LiF calibration crystal. At room temperature, the (200) Bragg plane of LiF is a nearly 100% elastic scatterer of 46.5-keV γ rays[16,17] and so we can determine the recoilless fraction of the incident beam by scattering from LiF. The ratio of the recoilless fraction after scattering to the recoilless fraction before scattering is the elastic scattering fraction, and this, when multiplied by the total scattered intensity, determines the elastic intensity, and thus the DWF.

III. EXPANSION OF THE DEBYE-WALLER FACTOR

The exponential of the Debye-Waller factor can easily be expanded in a power series in Q and T. For cubic crystals with inversion symmetry, keeping only terms of order Q^4 or less, the DWF exponential can be written quite simply. To simplify calculations, we normalize our data to the intensity at room temperature and take the natural logarithm, to determine the exponential of the DWF. It is customary to divide out the Q^2 dependence of this exponential so that anharmonic effects may be more easily seen.

A typical function to which previous investigators have fit the integrated intensity measurements is given by[18–20]

$$Y = Y_H - (4\pi)^2[m_2T^2 + m_3T^3 + Q^2 m_4 T^3], \tag{2}$$

where the rescaled elastic intensities are given by

$$Y = \frac{(4\pi)^2}{Q^2} \ln \frac{I}{I_0}. \tag{3}$$

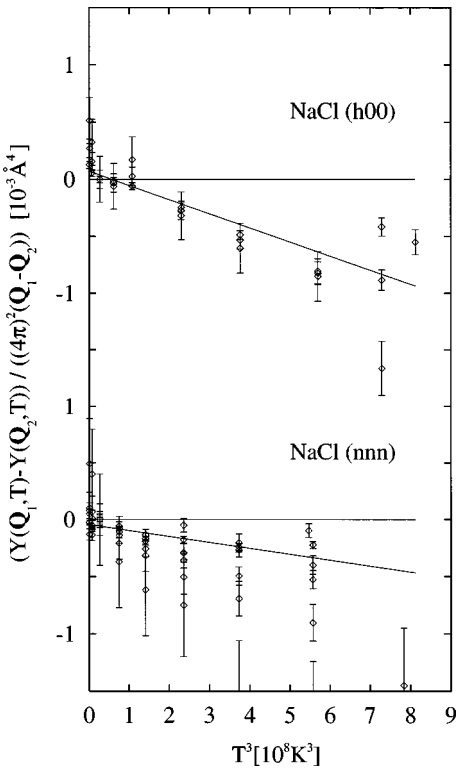

FIG. 3. A plot of the Q^4 contribution to the Debye-Waller factor. The slope of each line corresponds to the m_4 coefficient. Q_1 and Q_2 are two different scattering wave vectors which have the same direction.

I and I_0 are the integrated elastic intensities at the temperature T and at the reference temperature, respectively. The harmonic term Y_H is given by

$$Y_H = C - \left(\frac{12h^2}{mk_B\Theta_D^2} \right) T\Psi\left(\frac{\Theta_D}{T} \right), \tag{4}$$

where

$$\Psi(x) = \frac{1}{x}\int_0^x \frac{z\,dz}{e^z - 1},$$

C is a constant and a parameter in the fitting process, m is the mean ionic mass, k_B is the Boltzmann constant, and h is the Planck constant. m_2, m_3, and m_4 are the anharmonic terms of interest, and Θ_D is the Debye temperature. By direct comparison of parallel reflections, the value of m_4 can be determined independently of the other parameters (see Fig. 3), but the others must be found by fitting the data for the remaining four simultaneously. This presents a problem because all but C are highly correlated. This problem has been ignored in the past by simply selecting a value for the Debye temperature, ignoring m_3 or carrying out some thermal expansion corrections, and fitting only for m_2 and m_4, which is determined as above. We reduced the problem greatly by correcting our measured intensities for the thermal expansion of the sample crystals. Both m_2 and m_3 are associated with thermal expansion. m_2 contains a part from thermal expansion, but other factors also contribute. m_3 is wholly due to the nonlinearity of thermal expansion with temperature. If the intensities of the reflections are corrected for thermal expansion, $m_3 = 0$.[21] By using thermal expansion data[22–24] to correct our data for the changes in Q, the Lorentz polarization factor, and the number of scattering centers in the γ-ray beam, we eliminated m_3.

After eliminating m_3 from the analysis by correcting for thermal expansion, we can fit our data to the function

$$Y = Y_H - (4\pi)^2[m_2T^2 + Q^2m_4T^3], \tag{5}$$

which is the same as Eq. (2) when $m_3 = 0$. We first determine m_4 by a direct comparison of reflections within a family, independently of the other parameters. By writing Eq. (5) for two different reflections with Y values given by Y_1 and Y_2, we can eliminate the harmonic and m_2 terms if we take the difference between them. This gives us

$$Y_1 - Y_2 = C_1 - C_2 - (4\pi)^2Q_1^2m_4T^3 + (4\pi)^2Q_2^2m_4T^3, \tag{6}$$

where C_1 and C_2 are the constant terms in Eq. (4) for the two different reflections. The terms with m_2 and Θ_D drop out because they do not depend on the magnitude of Q, and so they are the same for each reflection. From this it can be seen that a plot of $(Y_1 - Y_2)/[(4\pi)^2(Q_1^2 - Q_2^2)]$ versus T^3 will have a slope of $-m_4$. After determining m_4 we fit for all other parameters simultaneously.

IV. THERMAL-EXPANSION CORRECTIONS

We have investigated the use of the parameter m_3, and we find that the results obtained when using it with intensity data not corrected for thermal expansion are in error. The correction for the number of scattering centers is independent of $\vec{Q}$, which means that the correction to the Y values depends on $\vec{Q}$. The corrected Y values differ from the uncorrected Y values by large amounts for low-order reflections, while the difference is much smaller for the (600) reflections. This can be clearly seen in Fig. 4. Because this difference in Y values varies dramatically with Q, a failure to properly account for these thermal-expansion effects makes it impossible to correctly determine m_4.

The thermal-expansion corrections to the Y values from changes in $\vec{Q}$, from the explicit dependence on Q and from the change in the Lorentz polarization term which is due to its explicit Q dependence, are straightforward. The change in the number of scattering centers is more complicated. Our crystals expand in three dimensions, length, depth, and height. The expansion in depth of the crystal does not affect the number of scattering sites, because the penetration depth of the γ rays increases as well. The net effect of this expansion is to broaden the scattered beam slightly. In these experiments, the collimation at the detector was such that the entire broadened beam was still accepted into the detector. Consequently, the expansion in this dimension did not cause a change in the intensity of the scattered beam.

The originally selected crystals are all taller than the height of the beam, and so as they expand the number of scattering sites decreases. Likewise, the crystals are longer than the effective beam width on the face of the crystal, and again as they expand in this direction, the number of scattering sites decreases. These two combine to give a two-

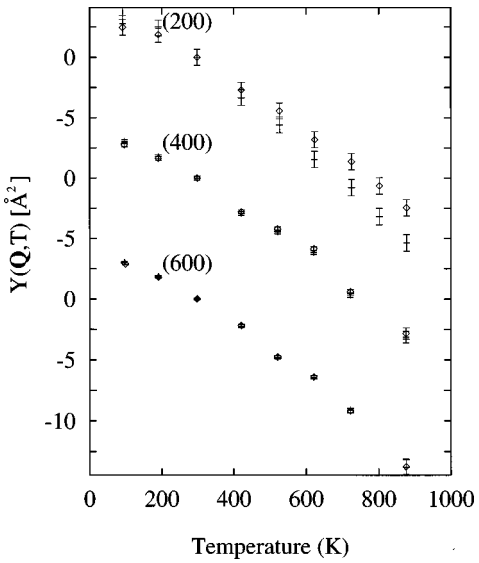

FIG. 4. A plot of the rescaled elastic intensities $Y(\vec{Q},T)$ vs temperature for KBr showing the difference between the expansion corrected and uncorrected Y values. The uncorrected data are the diamonds; the corrected data are the pluses.

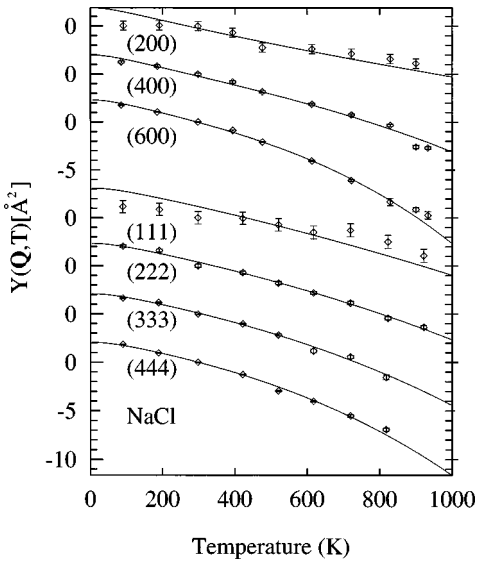

FIG. 5. A plot of $Y(\vec{Q},T)$ vs temperature for NaCl. The scale for each curve is the same.

dimensional correction to the scattered intensity. However, we also used two smaller crystals (KCl), for which the crystal was smaller than the beam in both of these directions. In these cases, we made no correction for a change in the number of scattering sites. The (111) and (200) reflections on the larger crystals are potential problems. If the crystals are correctly oriented, the crystals are longer than the beam; however, if the crystal is slightly misaligned, the beam may be wider than the length of the crystal. In this case, a one-dimensional correction would be more appropriate. This may have been the case with NaCl. The uncertainties on these low-angle data points are such that the fitted parameters are not affected by which correction is made. However, the one-dimensional correction gives a result with a slightly smaller χ^2.

To make these thermal expansion corrections correctly, it is essential to know the variation of the lattice constants with temperature. The coefficient of thermal expansion is not constant at either low temperature or high temperature, and so using the room temperature value, as has been done in the past, leads to large errors. Since the lattice constants of all three of these alkali halides have been measured as a function of temperature over the entire range of this experiment, we have used these experimental values instead. We used the fitting functions of Pathak *et al.* to calculate the lattice constants at each measured temperature.[22–24] We then calculated $Q(T)$ and the relative number of scattering sites illuminated using these lattice constants.

V. RESULTS AND DISCUSSION

We took our measured elastic scattering intensities, corrected them for thermal expansion, and converted them into Y values to more readily see anharmonic effects. The experimental Y values and the curves fitted to these points for NaCl, KCl, and KBr are shown in Figs. 5–7, respectively. The lowest-order reflections deviate most from the curves due to the alignment difficulties discussed earlier. Additionally, notice that the error bars (1σ statistical errors) are much larger on the low-order reflections than the high-order reflections. This is a consequence of the definition of the Y's. The actual elastic intensities were found to greater precision in the case of the low-order reflections, but to determine the Y values we must divide by Q^2. This reduces the uncertainty in the high-order Y's.

To fit our data to Eq. (5), even after independently determining m_4, it was necessary to place constraints on the parameters Θ_D and m_2. The correlation between these parameters was so large that fitting the data from a single reflection gave uncertainties greater than the value of the parameter. It was essential to fit several reflections simultaneously. The Debye temperature and m_2 were thought to be fixed for a given crystal, not varying with $\vec{Q}$.[21,25,26] The Debye temperature was thought to vary as $1/\sqrt{\text{mass}}$, from Eq. (4) and because the phonon spectra of these three crystals are almost

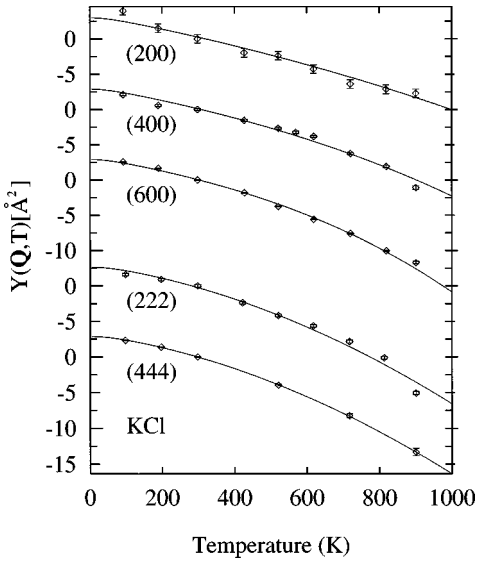

FIG. 6. A plot of $Y(\vec{Q},T)$ vs temperature for KCl.

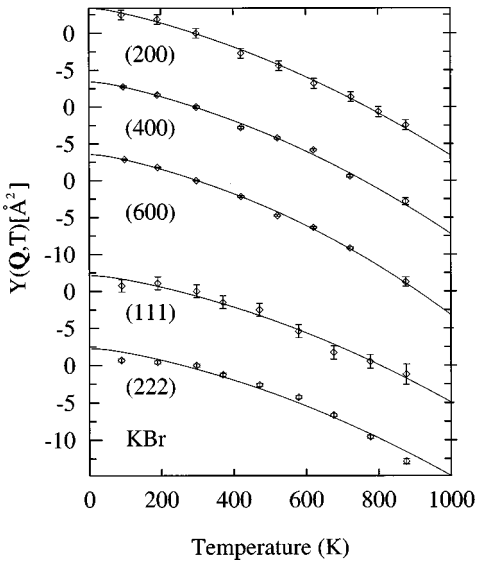

FIG. 7. A plot of $Y(\vec{Q},T)$ vs temperature for KBr.

identical, differing by only a scaling factor. We tested these assumptions to determine how best to constrain our parameters.

We discovered that it was not possible to fit the two different sets of reflections with the same Debye temperature and m_2. While this reduced the uncertainties in the parameters, the fitted curves did not correspond to the data. This is seen in Figs. 8 and 9, and this effect is even more pronounced for KCl.[27] When they are constrained to have the same Θ_D and m_2, the $(h00)$ data and the (nnn) data move away from the fitted curve in opposite directions as the temperature increases. We can, however, constrain Θ_D and m_2 to be the same for each reflection in a family [that is, for the (200), (400), and (600) reflections we can require that they be the same]. This causes no problems in fitting the data.

Within errors, the values for the Debye temperature found

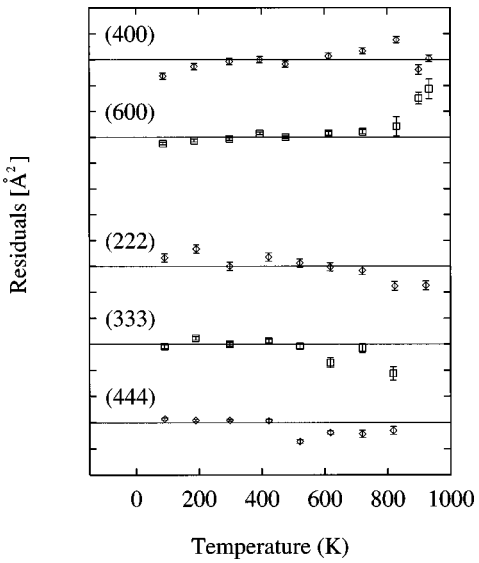

FIG. 8. A residual plot for NaCl showing the poor fit obtained when requiring Θ_D and m_2 to be the same for both sets of reflections. Each vertical division is 1 Å. Notice that the $(h00)$ points slope up while the (nnn) points slope down.

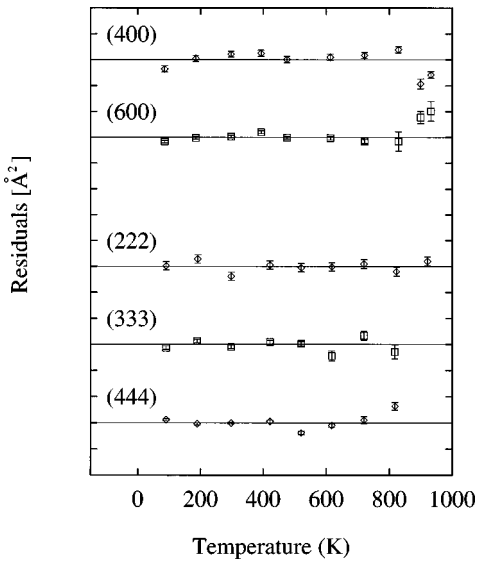

FIG. 9. A residual plot for NaCl showing the better fit obtained when allowing Θ_D and m_2 to be different for the two sets of reflections. Each vertical division is 1 Å.

for each crystal varied according to $1/\sqrt{\text{mass}}$, where the mass referred to here is the mean ionic mass of the alkali-halide crystal for each of the three crystals studied. The values for the two different directions were different, but both sets of reflections followed this relationship. Therefore, we made this a constraint in our fitting process. We fit all our $(h00)$ data together, allowing the m_2 values to vary independently from one crystal to another but requiring the Debye temperatures to vary according to the reciprocal of the square root of the mean ionic mass. We fit our (nnn) data in the same manner. Three important points were revealed by these analyses and are discussed below.

The first is that the Debye-Waller factor varies with crystal orientation in these cubic crystals. All three of the nontrivial parameters determined in our data fitting process, the Debye temperature and the two anharmonic constants m_2 and m_4, varied with crystal orientation. The difference in the Q^4 contribution was not unexpected, but because these crystals all have cubic symmetry, it is believed that the Debye temperature and the Q^2T^2 term will be the same for the $[h00]$ and the $[nnn]$ directions or, in fact, for any direction.[21,25,26] The mean-square displacement of an ion is the same in any direction, and so the Debye temperature and m_2 must be identical for the different directions. This is not the case. The coefficient m_2 differs between the two directions, tending to be larger in the $[nnn]$ direction ($m_2 = 7.6(5)\times10^{-8}$ Å^2/K^2 in the $[nnn]$ direction versus $m_2 = 1.7(4)\times10^{-8}$ Å^2/K^2 in the $[h00]$ direction for KCl). The Debye temperatures in the $[nnn]$ direction were 14(5)% larger than in the $[h00]$ direction. A larger Debye temperature implies a smaller mean-square displacement from equilibrium; a larger m_2 implies a larger mean-square displacement from equilibrium, although this term is a lesser contribution to the mean-square displacement, especially at low temperatures.

These results indicate that at lower temperatures, the ions oscillate with a larger amplitude in the $[h00]$ direction than in the $[nnn]$ direction. Thus, the probability density for the

TABLE I. Debye-Waller factor parameters. The parenthetical quantity associated with each number is the error in the last figure of the measured quantity. When two digits are given in parentheses, e.g., $\Theta_D = 283(18)$, we mean $\Theta_D = 283 \pm 18$.

Crystal	Direction	Θ_D (K)	m_2 (Å^2/K^2)	m_4 (Å^4/K^3)
NaCl	$(h00)$	281(7)	$-1.4(4) \times 10^{-8}$	$11.2(9) \times 10^{-13}$
NaCl	(nnn)	320(13)	$1.4(5) \times 10^{-8}$	$4.1(8) \times 10^{-13}$
KCl	$(h00)$	249(6)	$2.5(4) \times 10^{-8}$	$10(2) \times 10^{-13}$
KCl	(nnn)	283(18)	$8.0(5) \times 10^{-8}$	$-3(3) \times 10^{-13}$
KBr	$(h00)$	197(5)	$7.3(5) \times 10^{-8}$	$1(2) \times 10^{-13}$
KBr	(nnn)	224(10)	$6.8(6) \times 10^{-8}$	—

ions is not spherically symmetric; at low temperatures the mean-square radius may change by as much as 30% from $[nnn]$ to $[h00]$. As the temperature is increased, m_2 contributes more, and so the oscillation of the ions becomes more spherical. For KBr, where the values of m_2 are nearly equal in the two directions, the asymmetry remains large up to high temperatures. For NaCl and KCl, where the values of m_2 are very different in the two directions studied, the asymmetry decreases with increasing temperature. In general, our results indicate that the thermal cloud of the ions is not spherically symmetrical in these cubic crystals, and the asymmetry diminishes with increasing temperature.

The general assumption has been that in cubic crystals like these, where there is inversion symmetry about every ion, the vibration of the ions about their equilibrium points is spherically symmetric. This is an unstated assumption in most discussions of Debye-Waller factors and most measurements of it. It follows from the more general notion that the thermal cloud is an ellipsoid, and in cubic crystals where $\langle x^2 \rangle = \langle y^2 \rangle = \langle z^2 \rangle$ it follows that the thermal cloud must have spherical symmetry. Thus a single Debye temperature is given for a material, independent of the direction of scattering. Our results demonstrate that there is a difference in the Debye-Waller factors for different directions within a crystal and that the thermal cloud is not spherically symmetric.

The second point is that we do observe a Q^4 contribution to the DWF. Earlier measurements[1,4,5] reported a Q^4 contribution but reported coefficients varied by two orders of magnitude, discrepancies that are so large as to shed doubt on these earlier claims of a nonvanishing Q^4 term. All the reported values are larger than our data indicate. In KCl we find $m_4 = 1.1(2) \times 10^{-12}$ Å^4/K^3, while Martin and O'Connor[1] report a value of $m_4 = 4(1) \times 10^{-12}$ Å^4/K^3 and Solt *et al.*[5] report $m_4 = 1.5(6) \times 10^{-10}$ Å^4/K^3. These earlier measurements were limited by a low source intensity, which forced them to make compromises in the data collection and analysis, and it is unclear how, if at all, they accounted for thermal expansion.

Our high-photon-intensity measurements allow us to draw a definitive conclusion that there is a Q^4 contribution at these temperatures for NaCl and KCl. The evidence for such a Q^4 dependence in the KBr samples is not compelling ($m_4 = 4(2) \times 10^{-13}$ Å^4/K^3 for the $[h00]$ direction, and $m_4 = 4(2) \times 10^{-12}$ Å^4/K^3 for the $[nnn]$ direction, when m_4 is determined by a simultaneous fit with m_2 and Θ_D); however, it suggests that there is such a dependence and that in the $[nnn]$ direction it may be quite large. In the KCl samples, the $[nnn]$ reflections also show no Q^4 dependence within errors [$m_4 = 1(30) \times 10^{-14}$ Å^4/K^3]; however, the $[h00]$ reflections do show such a dependence [$m_4 = 1.1(2) \times 10^{-12}$ Å^4/K^3]. Both sets of reflections show a Q^4 dependence for the NaCl samples; however, the coefficient is significantly larger in the $[h00]$ direction ($h00$, $m_4 = 1.2(1) \times 10^{-12}$ Å^4/K^3; nnn, $m_4 = 5.2(8) \times 10^{-13}$ Å^4/K^3). These values are listed in Table I.

The third point is that the (nnn) reflections with all odd indices and the (nnn) reflections with all even indices have the same temperature dependence. If measurements of the intensity for both even and odd ordered (nnn) reflections are made, it is possible to separate the scattering of the two types of ions, and measure individual DWF's for the ions. We can write the scattered intensity for each type of reflection in two ways, once using an average DWF and once using an individual DWF for cations and anions separately, as Martin and O'Connor did.[1] The total scattering can be written in terms of an average Debye-Waller factor as

$$I_{\text{sum}} = Ep(\Theta)|[f_1(\vec{Q}) + f_2(\vec{Q})]e^{-M_S(\vec{Q},T)}|^2 \tag{7}$$

for the even-order reflections and

$$I_{\text{diff}} = Ep(\Theta)|[f_1(\vec{Q}) - f_2(\vec{Q})]e^{-M_D(\vec{Q},T)}|^2 \tag{8}$$

for the odd-order reflections. It can also be written in terms of the separate Debye-Waller factors as

$$I_{\text{sum}} = Ep(\Theta)|f_1(\vec{Q})e^{-M_1(\vec{Q},T)} + f_2(\vec{Q})e^{-M_2(\vec{Q},T)}|^2 \tag{9}$$

for the even-order reflections and

$$I_{\text{DIFF}} = Ep(\Theta)|f_1(\vec{Q})e^{-M_1(\vec{Q},T)} - f_2(\vec{Q})e^{-M_2(\vec{Q},T)}|^2 \tag{10}$$

for the odd-order reflections. In these equations E is an intensity term which depends only on the incident intensity and $p(\Theta)$ is an angular-dependent term which takes into account polarization and the volume of the crystal irradiated. I_{sum} is-

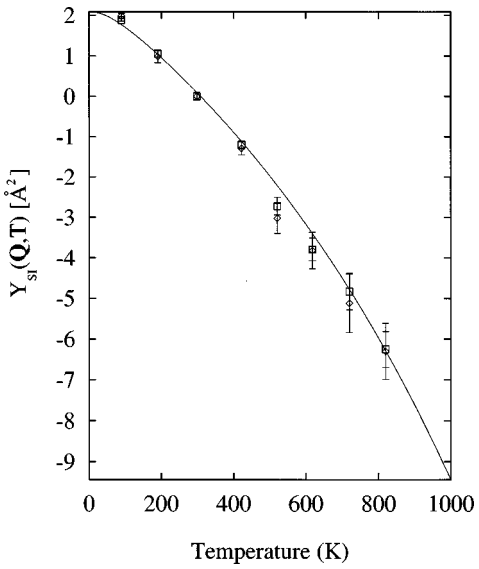

FIG. 10. A plot of the rescaled single-ion elastic intensity $Y_{SI}(\vec{Q},T)$ vs temperature for the separate ion types in NaCl. The diamonds are the cation data and the pluses are the anion data.

the intensity when the reflections from the two types of atoms are in phase, and I_{diff} is the intensity when the reflec tions from the two types of atoms are out of phase. For the rocksalt structure, scattering from the (nnn) planes depends on the sum of the scattering from the alkali and halide ions when n is even and the difference when n is odd, and so the DWF for the individual ions, $e^{-2M_1(\vec{Q},T)}$ and $e^{-2M_2(\vec{Q},T)}$, may be calculated from data from the (nnn) planes. Referencing all intensities to room temperature and using known atomic scattering factors f,[28] and our measured intensities for the (nnn) reflections, we fit all our (nnn) data simultaneously to the individual Debye-Waller factors. We had data for the (111), (222), (333), and (444) reflections for NaCl, and the (111) and (222) reflections for KBr. The data for NaCl clearly show that the different ions have the same temperature dependence. For KBr the results are not as clear, due to the larger uncertainties in these measurements, but they are consistent with this hypothesis. Figure 10 shows the Y values for the single-ion scattering, Y_{SI}, for NaCl.

These results are in contrast to earlier measurements by Martin and O'Connor,[1] who claimed to have seen different temperature dependences for the individual ions. Their measurements, however, suffered from the ^{57}Fe experimental drawbacks associated with inadequate photon intensities, and they did not correctly account for thermal expansion effects. Additionally, they did not directly determine the single-ion scattering; they attempted to estimate what the scattering would be in certain cases and used these estimates to determine the single-ion scattering. Given the systematic errors introduced in their experiments and the contrast in intensity between the all-odd and the all-even reflections, the difference between our results and their claims is not surprising.

The identical DWF's for the two ion types require that the mean-square displacements of the ions be identical in the $[nnn]$ direction. For temperatures above the Debye temperature, this is expected.[25,29,30] The bulk of our measurements were taken at high temperatures, as we were primarily interested in anharmonic effects. The amount and quality of data taken below the Debye temperature of each sample were insufficient to allow any conclusions to be drawn about the relative DWF's of the two ion types at low temperatures. If one considers the system in the light of the equipartition theorem as has Disatnik *et al.*,[31] it becomes clear that the amplitudes of vibration for the two types of ions should be the same at high temperature. By equipartition, the average kinetic energies of the two ion types should be equal, and thus the average potential energies of the two should be equal. The potential energy for a particle on a spring is given by $\frac{1}{2}ku^2$, and since the two ions share the same spring constant k, they will have the same mean-square displacement, whenever the temperature is high enough for the equipartition theorem to hold. At low temperatures, where equipartition would not be valid, the change in scattered intensity with temperature is too small to allow us to see any differences between the scattering from the two types of ions in this experiment.

VI. CONCLUSION

In conclusion, we have carefully collected Debye-Waller factor data for NaCl, KCl, and KBr, and corrected them for the thermal-expansion of each crystal. The thermal-expansion corrections are absolutely essential for a proper analysis of the data, and must be made with care. Accurate lattice constant data over the entire temperature range are needed, as the expansion of these crystals is complicated. One must correct for three effects, the change in Q in the definition of the rescaled elastic intensities [the Y values defined in Eq. (3)], the change in Q in the Lorentz polarization factor, and the number of scattering sites illuminated by the gamma beam.

We find that the Debye temperatures and the anharmonic coefficients vary with the mean ionic mass, such that the Debye temperature varies according to $1/\sqrt{\text{mean mass}}$ and m_2 increases with increasing mass. In the $(h00)$ direction m_4 decreases with increasing mean mass, though the functional dependence is not apparent, while in the (nnn) direction our data do not indicate a systematic change in m_4 with mean mass. The reasons for the dependence of m_4 on mass are not yet understood. We find that there is a quartic term in the DWF exponent (m_4 is nonzero), but that it is much smaller than earlier reports had indicated. This dependence is obvious in the cases of NaCl and KCl, but less convincing for KBr because of our large experimental errors in this latter case.

We have determined that the two types of ions in these crystals have the same mean-square displacement from equilibrium, as would be expected at high temperatures from the equipartition theorem. This supports claims by Huiszoon and Groenewegen[29] and Jex *et al.*[30] that, for temperatures greater than the Debye temperature and in the harmonic approximation, the mean-square displacements of ions are independent of their masses.

We have found that the Debye temperature and the coefficient m_2 do vary with direction, indicating that the oscillations of the ions about their equilibrium positions are not spherically symmetric. It is generally accepted that the ther-

mal cloud is isotropic for cubic crystals with inversion symmetry about each atom. This experiment does not support this belief. The data clearly show DWF's which are different in the two directions studied here, leading us to the conclusion that the ions have different amplitudes of oscillation in the two directions. This latter result shows that in general the shape of the thermal cloud is not ellipsoidal as crystallographers have thought.

ACKNOWLEDGMENTS

This work was prepared with the support of the U.S. Department of Energy, Grant No. DE-FG02-85 ER 45199 and NSF Grant No. DMR-9623684 and is taken from the Ph.D. thesis work of Carmen K. Shepard of Purdue University. C.K.S. thanks the Purdue Research Foundation for providing financial support for the purpose of carrying out this thesis research.

*Current address: Maysville Community College, Maysville, Kentucky 41056.

[1] C. J. Martin and D. A. O'Connor, Acta Crystallogr., Sect. A: Cryst. Phys., Diffr., Theor. Gen. Crystallogr. **34**, 505 (1978).
[2] G. Albanese, C. Ghezzi, and A. Merlini, Phys. Rev. B **7**, 65 (1973).
[3] N. M. Butt and D. A. O'Connor, Proc. Phys. Soc. London **90**, 247 (1966).
[4] N. M. Butt and G. Solt, Acta Crystallogr., Sect. A: Cryst. Phys., Diffr., Theor. Gen. Crystallogr. **27**, 238 (1971).
[5] G. Solt, N. M. Butt, and D. A. O'Connor, Acta Crystallogr., Sect. A: Cryst. Phys., Diffr., Theor. Gen. Crystallogr. **29**, 228 (1973).
[6] K. Krec and W. Steiner, Acta Crystallogr., Sect. A: Found. Crystallogr. **40**, 459 (1984).
[7] W. B. Yelon, G. Schupp, M. L. Crow, C. Holmes, and J. G. Mullen, Nucl. Instrum. Methods Phys. Res. B **14**, 323 (1986).
[8] J. G. Mullen, A. Djedid, D. Cowan, G. Schupp, M. L. Crow, Y. Cao, and W. B. Yelon, Phys. Lett. B **127**, 242 (1988).
[9] B. Bullard, J. G. Mullen, and Guy Schupp, Phys. Rev. B **43**, 7405 (1991).
[10] B. R. Bullard and J. G. Mullen, Phys. Rev. B **43**, 7416 (1991).
[11] R. A. Wagoner, B. Bullard, J. G. Mullen, and G. Schupp, Hyperfine Interact. **77**, 71 (1993).
[12] R. A. Wagoner, J. G. Mullen, and G. Schupp, Phys. Lett. B **279**, 25 (1992).
[13] S. N. Dickson, J. G. Mullen, and R. D. Taylor, Hyperfine Interact. **93**, 1445 (1994).
[14] S. N. Dickson, Ph.D. thesis, Purdue University, 1995.
[15] R. A. Wagoner, B. Bullard, M. May, S. Dickson, and J. G. Mullen, Hyperfine Interact. **58**, 2687 (1990).
[16] J. G. Mullen and J. R. Stevenson, in *Workshop on New Directions in Mössbauer Spectroscopy*, edited by G. J. Perlow, AIP Conf. Proc. No. 38 (AIP, New York, 1997), p. 55.
[17] J. G. Mullen, R. A. Wagoner, and G. Schupp, Hyperfine Interact. **83**, 147 (1994).
[18] G. A. Wolfe and B. Goodman, Phys. Rev. **187**, 1171 (1969).
[19] A. A. Maradudin and P. A. Flinn, Phys. Rev. **129**, 2529 (1963).
[20] G. A. Heiser, R. C. Shukla, and E. R. Cowley, Phys. Rev. B **33**, 2158 (1986).
[21] B. T. M. Willis, Acta Crystallogr., Sect. A: Cryst. Phys., Diffr., Theor. Gen. Crystallogr. **25**, 277 (1968).
[22] P.D. Pathak and N. G. Vasavada, Acta Crystallogr., Sect. A: Cryst. Phys., Diffr., Theor. Gen. Crystallogr. **26**, 655 (1970).
[23] P.D. Pathak, J.M. Trivedi, and N.G. Vasavada, Acta Crystallogr., Sect. A: Cryst. Phys., Diffr., Theor. Gen. Crystallogr. **29**, 477 (1973).
[24] K. E. Salimäki, Ann. Acad. Sci. Fenn., AVI No. **56** (1960).
[25] N. M. Butt, J. Bashir, and M. Nasir Khan, Acta Crystallogr., Sect. A: Found. Crystallogr. **49**, 171 (1993).
[26] R. W. James, *The Optical Principles of the Diffraction of X-rays* (Bell, London, 1967).
[27] C. K. Shepard, J. G. Mullen, and G. Schupp, Hyperfine Interact. (to be published).
[28] International Union of Crystallography, *International Tables for X-Ray Crystallography* (The Kynock Press, Birmingham, 1962), Vol. 3, pp. 201–207.
[29] G. Huiszoon and P. P. M. Groenewegen, Acta Crystallogr., Sect. A: Cryst. Phys., Diffr., Theor. Gen. Crystallogr. **28**, 170 (1972).
[30] H. Jex, M. Mullner, and W. Dyck, Phys. Status Solidi B **61**, 241 (1974).
[31] Y. Disatnik, D. Fainstein, and H. J. Lipkin, Phys. Rev. **139**, A292 (1965).